Inorg. Chem. **2002**, *41*, 5364–5372

Trigonal Bipyramidal Geometry and Tridentate Coordination Mode of the Tripod in $FeCl_2$ Complexes with Tris(2-pyridylmethyl)amine Derivatives Bis-α-Substituted with Bulky Groups. Structures and Spectroscopic Comparative Studies

Dominique Mandon,*,† Ahmed Machkour,† Sandrine Goetz,† and Richard Welter‡

Laboratoire de Chimie Organométallique et de Catalyse and Laboratoire DECMET, UMR CNRS No. 7513, Université Louis Pasteur, Institut Le Bel, 4 rue Blaise Pascal, F-67070 Strasbourg Cedex, France

Received October 23, 2001

A series of dichloroferrous complexes with ligands derived from the tris(2-pyridylmethyl)amine tripod has been prepared and characterized. The X-ray crystal structures of the complexes [bis(2-bromo-6-pyridylmethyl)(2-pyridylmethyl)amine]$Fe^{II}Cl_2$ ($(Br_2TPA)Fe^{II}Cl_2$) and [bis(2-phenyl-6-pyridylmethyl)(2-pyridylmethyl)amine]$Fe^{II}Cl_2$, ($(Ph_2$-TPA)$Fe^{II}Cl_2$) are reported. In these complexes, the tripod coordinates in the tridentate mode, with a substituted pyridyl arm dangling away from the metal. Both complexes have a trigonal bipyramidal iron center with two equatorial chloride ions. Their crystal structures are compared with those of the [tris(2-pyridylmethyl)amine]$Fe^{II}Cl_2$ and [(2-bromo-6-pyridylmethyl)bis(2-pyridylmethyl)amine]$Fe^{II}Cl_2$ complexes ($(TPA)Fe^{II}Cl_2$ and $(BrTPA)Fe^{II}Cl_2$, respectively) in which the ligand coordinates in the tetradentate mode. For all complexes, the metal to ligand distances are systematically above the value of 2.0 Å, and ^1H NMR displays paramagnetically shifted resonances with short relaxation times. This indicates that the iron is in a high-spin state. Electric conductivity measurements show that, for all complexes, the measured values lie within the same range, significantly below those expected for ionic complexes. Together with the analysis of the UV–visible and NMR data, this strongly suggests that the coordination mode of the tripod is retained in solution.

Introduction

Iron complexes of the tetradentate tripodal ligand TPA (tris(2-pyridylmethyl)amine) and its derivatives have been over the past 10 years extensively studied because of their ability to mimic some structure and function patterns of non-heme iron monooxygenases or oxygen-activating enzymes.[1] In most of the cases in the chemistry of synthetic analogues of such metalloproteins, hydroperoxides are used as oxygen-donating reagents.[2−5] On the other hand, the biomimetic use of molecular dioxygen involves in general reaction with ferrous compounds or, in some cases, the presence of ferric ions together with easily reduced substrates or reducing agents.[6−9] This topic has been reviewed several times from both chemical and biological points of view, and many reaction pathways and intermediates have been examined in detail.[10−12] Thus many examples of ferrous complexes, potential candidates for reactivity studies with dioxygen, have been described, for which in most of the cases the usual

* Author to whom correspondence should be sent. E-mail: mandon@chimie.u-strasbg.fr. Phone: 33-(0)390-241-537. Fax: 33-(0)390-245-001.
† Laboratoire de Chimie Organométallique et de Catalyse.
‡ Laboratoire DECMET.

(1) Que, L., Jr.; Dong, Y. *Acc. Chem. Res.* **1996**, *29*, 190−196.
(2) Hsu, H.-F.; Dong, Y.; Shu, L.; Young, V. G.; Que, L., Jr. *J. Am. Chem. Soc.* **1999**, *121*, 5230−5237.
(3) Zang, Y.; Kim, J.; Dong, Y.; Wilkinson, E. C.; Appelman, E.; Que, L., Jr. *J. Am. Chem. Soc.* **1997**, *119*, 4197−4205.
(4) Que, L., Jr.; Chen, K. *J. Am. Chem. Soc*. **2001**, *123*, 6327−6337.
(5) Miyake, H.; Chen, K.; Lange, S. J.; Que, L., Jr. *Inorg. Chem*. **2001**, *40*, 3534−3538.
(6) Chiou, Y.-M.; Que, L., Jr. *J. Am. Chem. Soc*. **1995**, *117*, 3999−4013.
(7) Menage, S.; Zang, Y.; Hendrich, M. P.; Que, L., Jr. *J. Am. Chem. Soc*. **1992**, *114*, 7786−7792.
(8) Kryatov, S. V.; Rybak-Akimova, E. V.; MacMurdo, V. L.; Que, L., Jr. *Inorg. Chem.* **2001**, *40*, 2220−2228.
(9) Funabiki, T.; Yamazaki, T.; Fukui, A.; Tanaka, T.; Yoshida, S. *Angew. Chem., Int. Ed*. **1998**, *37*, 513−515.
(10) Solomon, E. I.; Brunold, T. C.; Davis, M. I.; Kemsley, J. N.; Lee, S.-K.; Lehnert, N.; Neese, F.; Skulan, A. J.; Yang, Y. S.; Zhou, J. *Chem. Rev.* **2000**, *100*, 235−349.
(11) Shu, L.; Nesheim, J. C.; Kauffmann, K.; Münck, E.; Lipscomb, J. D.; Que, L., Jr. *Science* **1997**, *275*, 515−518.
(12) Wallar, B. J.; Lipscomb, J. D. *Chem. Rev.* **1996**, *96*, 2625−2657.

10.1021/ic011104t CCC: $22.00 © 2002 American Chemical Society
Published on Web 09/19/2002

hexacoordination around the metal is observed.[13−17] With respect to coordination of molecular dioxygen to the metal center, it seems obvious that, together with electronic factors, the geometry around the metal plays a crucial role. We are thus trying to build up simple complexes in which some TPA derivatives would coordinate a ferrous ion leaving the metal coordinatively unsaturated. With TPA ligands monosubstituted in the α position of one of the pyridyl arms by a bulky group, bromine atom, or phenyl substituent, we have reported the preparation of trichloro ferric complexes.[18] We showed that steric hindrance on the substituted pyridine, associated with the good affinity of chloride ions for the metal, induces in that case tridentate coordination of the tripod to $FeCl_3$. The uncoordinated arm is the substituted pyridine, and the geometry is retained in solution. These high-spin compounds are very stable, and in that case the metal remains six-coordinate.

We have now extended our efforts to dichloroferrous compounds and found that both the parent TPA and the ligand brominated in the α position of *one* pyridyl arm coordinate in $LFeCl_2$ complexes in the usual tetradentate mode. However, with disubstituted ligands, i.e., when the α position of *two* of the three pyridyl arms is substituted, one of the substituted pyridyl arms is pushed away from the coordination site, leaving open a free position around the metal which becomes five-coordinate. The tripod then coordinates in the tridentate mode. We report herein, together with their UV−visible and ^{1}H NMR spectroscopic data, the crystal structures of the complexes [tris(2-pyridylmethyl)-amine]$Fe^{II}Cl_2$, L_1FeCl_2; [(2-bromo-6-pyridylmethyl)bis(2-pyridylmethyl)amine]$Fe^{II}Cl_2$, L_2FeCl_2; [bis(2-bromo-6-pyridylmethyl)(2-pyridylmethyl)amine]$Fe^{II}Cl_2$, L_3FeCl_2; and [bis(2-phenyl-6-pyridylmethyl)(2-pyridylmethyl)amine]Fe^{II}-Cl_2, L_4FeCl_2. Additionally, conductivity experiments have been carried out on the complexes, which show that they remain neutral in solution. Together with the analysis of the UV−visible and ^{1}H NMR data, this leads to the conclusion that the coordination mode observed in the solid state for each complex is retained in solution.

Experimental Section

The UV−vis spectra were recorded on a Varian Cary 05 E UV−vis NIR spectrophotometer. ^{1}H NMR data were recorded in CD_3-CN at ambient temperature on a Bruker AC 300 spectrometer at 300.1300 MHz using the residual signal of CD_2HCN as a reference for calibration. ^{2}H NMR data were recorded in CH_3CN at ambient temperature on a Bruker AVANCE 400 spectrometer at 61.4223910 MHz using the residual signal of CH_3CN as a reference for calibration.

Conductivity measurements were carried out under argon at 20 °C with a CDM 230 Radiometer Copenhagen conductivity meter, using a Tacussel XE 150 507569 electrode. Procedure used for the complexes: 4 mL of dry and degassed acetonitrile was introduced into the cell, and the relative conductivity of the blank was measured (*A*). Then the relative conductivity of the sample dissolved in 4 mL of the same solvent was measured (*B*). The conductivity of the compound is obtained by the subtraction $B - A$. The molar conductivity is the ratio $(B - A)$/concentration in complex. Procedure for $Fe^{II}(BF_4)_2 + L_{1-4}$: 4 mL of dry and degassed acetonitrile was introduced into the cell, and the relative conductivity of the blank was measured (*A*). Then a solution of $Fe^{II}(BF_4)_2$ dissolved in 4 mL of the same solvent was prepared. Two equivalents of ligand (L_{1-4}) was added, and a yellow color developed upon stirring. Five minutes later, the relative conductivity of the medium was measured (*C*). The conductivity of the compound is obtained by the subtraction $C - A$. The molar conductivity is the ratio $(C - A)$/concentration in iron.

Ligands L_1, L_2, and L_3 were prepared according to published methods.[19,20] L_4 was prepared from L_3 by adaptation of a published procedure using the Suzuki cross-coupling procedure.[20] ^{1}H NMR, $CDCl_3$, δ, ppm, TMS: 8.54, 1H d; 7.98, 4H m; 7.75−7.62, 4H m; 7.60−7.55, 4H m; 7.49−7.35, 6H m; 7.14, 1H m; 4.03, 4H s, 4.02, 2H s. MS, impact mode: $m/z = 442.15$. Elemental analysis for L_4: $C_{30}H_{26}N_4$. Calcd: C 81.45, H 5.88. Found: C 81.75, H 6.22. $[Ph_2d^{10}]L_4$ was prepared in a similar way from L_3 using $C_6D_5B(OH)_2$ from Aldrich Chemicals. ^{1}H NMR, $CDCl_3$, δ, ppm, TMS: 8.54, 1H d; 7.75−7.62, 4H m; 7.60−7.55, 4H m; 7.14, 1H m; 4.03, 4H s, 4.02, 2H s. MS, impact mode: $m/z = 452.23$.

Typical Metalation Experiment. All reactions were carried out with dry and degassed solvents under strict anaerobic conditions. Anhydrous $FeCl_2$ (0.9 equiv) in dry THF was added to a solution of ligand L_n in THF. The color immediately turned to orange-yellow, and the reaction medium was stirred for 2 h at room temperature. The solvent was removed under vacuum, and the solid was extracted with acetonitrile. After filtration and concentration, a yellow-orange solid was obtained by slow addition of diethyl ether, filtered off, washed with diethyl ether, and dried under vacuum. Further purification was achieved by diethyl ether crystallization from an acetonitrile solution. The yields are within the range 85−90%, and all compounds are thermally stable. In the crystalline form, the complexes can be rapidly handled under atmospheric conditions. Satisfactory elemental analyses could thus be obtained on the crystals. However, solutions of the complexes should be handled under anaerobic conditions.

X-ray Analysis. quantitative data were obtained at room temperature for $L_2Fe^{II}Cl_2$ and −100 °C for $L_1Fe^{II}Cl_2$, $L_3Fe^{II}Cl_2$, and $L_4Fe^{II}Cl_2$. All experimental parameters used are given in the Supporting Information. The resulting dataset was transferred to a DEC Alpha workstation, and for all subsequent calculations the Enraf-Nonius OpenMoleN package[21] was used.

The structure was solved using direct methods. After refinement of the heavy atoms, a difference Fourier map revealed maxima of residual electronic density close to the positions expected for hydrogen atoms; they were introduced as fixed contributors in structure factor calculations by their computed coordinates (C−H = 0.95 Å) and isotropic temperature factors such as $B(H) = 1.3$

(13) Diebold, A.; Hagen, K. S. *Inorg. Chem.* **1998**, *37*, 215−223.
(14) Zang, Y.; Que, L., Jr. *Inorg. Chem.* **1995**, *34*, 1030−1035.
(15) Zang, Y.; Jang, H. G.; Chiou, Y.-M.; Hendrich, M. P.; Que, L., Jr. *Inorg. Chim. Acta* **1993**, *213*, 41−48.
(16) Jo, D.-H.; Chiou, Y.-M.; Que, L., Jr. *Inorg. Chem.* **2001**, *40*, 3181−3190.
(17) Randall, C. R.; Shu, L.; Chiou, Y.-M.; Hagen, K. S.; Ito, M.; Kitajima, N.; Lachicotte, R. J.; Zang, Y.; Que, L., Jr. *Inorg. Chem.* **1995**, *34*, 1036−1039.
(18) Mandon, D.; Nopper, A.; Litrol, T.; Goetz, S. *Inorg. Chem.* **2001**, *40*, 4803−4806.
(19) Tyeklar, Z.; Jacobson, R. R.; Wei, N.; Murthy, N. N.; Zubieta, J.; Karlin, K. D.; *J. Am. Chem. Soc.* **1993**, *115*, 2677−2689.
(20) Chuang, C. L.; Dos Santos, O.; Xu, X.; Canary, J. W. *Inorg. Chem.* **1997**, *36*, 1967−1972.
(21) *OpenMoleN, Interactive Structure Solution*; Nonius B.V.: Delft, The Netherlands, 1997.

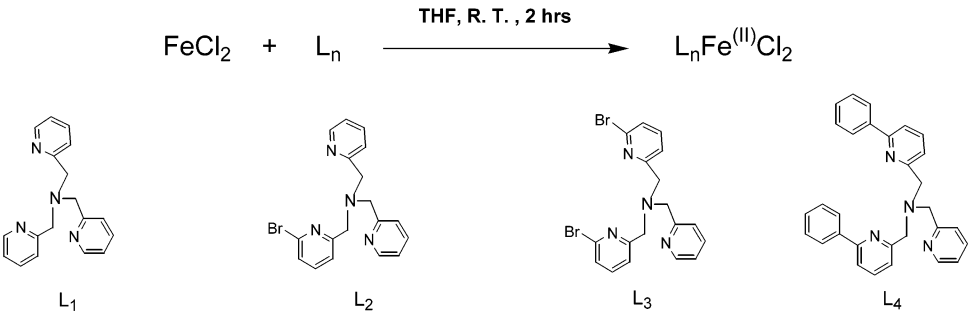

Figure 1. Ligands and complexes reported in this study.

B_{eqv}(C) Å^2 but not refined. Full least-squares refinements was on $|F|$. A final difference map revealed no significant maxima. The scattering factor coefficients and anomalous dispersion coefficients come respectively from refs 22a and 22b.

Crystal data for $L_1Fe^{II}Cl_2$: yellow crystals; crystal dimensions 0.15 × 0.13 × 0.10 mm^3; $C_{18}H_{18}N_4Cl_2Fe$, M = 417.12, orthorhombic, space group *Pbca*, a = 18.516(1) Å, b = 16.157(1) Å, c = 25.450 (1) Å, V = 7613(1) Å^3, Z = 16, D_c = 1.46 g cm^{-3}, μ(Mo Kα) = 1.082 mm^{-1}; a total of 16523 reflections, 2.5° < θ < 26.35°; 3842 independent reflections having $I > 3\sigma(I)$; 451 parameters. Final results: $R(F)$ = 0.041, $R_w(F)$ = 0.058, GOF = 1.183, maximum residual electronic density = 0.393 e Å^{-3}.

Crystal data for $L_2Fe^{II}Cl_2$: yellow crystals; crystal dimensions 0.10 × 0.09 × 0.08 mm^3; $C_{18}H_{17}N_4Cl_2BrFe$, M = 496.02, monoclinic, space group *Cc*, a = 9.3793(3) Å, b = 15.4229(6) Å, c = 14.3681 (6) Å, β = 104.284(2)°, V = 2014.18(13) Å^3, Z = 4, D_c = 1.64 g cm^{-3}, μ(Mo Kα) = 3.007 mm^{-1}; a total of 6290 reflections, 0.998° < θ < 30.034°; 3339 independent reflections having $I > 2\sigma(I)$; 235 parameters. Final results: $R(F)$ = 0.043, $R_w(F)$ = 0.104, GOF = 1.046, maximum residual electronic density = 0.727 e Å^{-3}.

Crystal data for $L_3Fe^{II}Cl_2$: orange crystals; crystal dimensions 0.19 × 0.16 × 0.11 mm^3; $C_{18}H_{16}N_4Cl_2Br_2Fe$, M = 574.93, monoclinic, space group $P2_1$, a = 8.4198(5) Å, b = 10.9214(8) Å, c = 11.3218(7) Å, β = 99.201(9)°, V = 1027.7(2) Å^3, Z = 2, D_c = 1.86 g cm^{-3}, μ(Mo Kα) = 4.859 mm^{-1}; a total of 7495 reflections, 2.5° < θ < 26.38°; 1511 independent reflections having $I > 3\sigma(I)$; 243 parameters. Final results: $R(F)$ = 0.034, $R_w(F)$ = 0.038, GOF = 1.022, maximum residual electronic density = 0.552 e Å^{-3}.

Crystal data for $L_4Fe^{II}Cl_2$: yellow crystals; crystal dimensions 0.20 × 0.08 × 0.06 mm^3; $C_{68}H_{66}N_{11}Cl_4Fe_2O_{0.5}$ = 2($C_{30}H_{26}N_4Cl_2$-Fe)·3(CH_3CN)·0.5($C_4H_{10}O$), M = 1306.86, triclinic, space group $P\bar{1}$, a = 9.1141(3) Å, b = 12.6745(7) Å, c = 15.6581(7) Å, α = 113.786(6)°, β = 94.924(6)°, γ = 91.108(6)°, V = 1646.1(3) Å^3, Z = 1, D_c = 1.32 g cm^{-3}, μ(Mo Kα) = 0.654 mm^{-1}; a total of 10310 reflections, 2.5° < θ < 27.46°; 4006 independent reflections having $I > 3\sigma(I)$; 382 parameters. Final results: $R(F)$ = 0.046, $R_w(F)$ = 0.075, GOF = 1.202, maximum residual electronic density = 0.657 e Å^{-3}.

Results

As with ferric complexes, the metalation of the ligands is simple and fast and proceeds smoothly in THF upon addition under argon of 1 equiv of $FeCl_2$ in solution to the corresponding ligand L (L_1 = tris(2-pyridylmethyl)amine, TPA; L_2 = (2-bromo-6-pyridylmethyl)bis(2-pyridylmethyl)amine, BrTPA; L_3 = bis(2-bromo-6-pyridylmethyl)(2-pyridylmethyl)amine, Br_2TPA; and L_4 = bis(2-phenyl-6-pyridylmethyl)(2-pyridylmethyl)amine, Ph_2TPA). Yellow to orange-yellow complexes are obtained almost quantitavely as L_n-$Fe^{II}Cl_2$ complexes, as shown in Figure 1. All compounds are thermally stable and are obtained in semiquantitative yield after workup. Slow diffusion of diethyl ether in acetonitrile solutions of the complexes yielded in each case crystals suitable for X-ray diffraction analysis.

Table 1. Selected Bond Lengths (Å) and Angles (deg) for the Six-Coordinate $L_nFe^{II}Cl_2$ Complexes

$L_1Fe^{II}Cl_2$				$L_2Fe^{II}Cl_2$	
a		*b*			
Fe1−Cl1	2.333(1)	Fe2−Cl4	2.340(1)	Fe−Cl1	2.4015(13)
Fe1−Cl2	2.465(2)	Fe2−Cl3	2.460(1)	Fe−Cl2	2.3604(12)
Fe1−N1	2.180(4)	Fe2−N8	2.196(4)	Fe−N1	2.302(4)
Fe1−N2	2.274(4)	Fe2−N6	2.266(4)	Fe−N2	2.169(4)
Fe1−N3	2.183(4)	Fe2−N7	2.199(4)	Fe−N3	2.248(4)
Fe1−N4	2.283(4)	Fe2−N5	2.203(4)	Fe−N4	2.354(4)
Cl1−Fe1−Cl2	100.99(6)	Cl3−Fe2−Cl4	99.03(5)	Cl1−Fe−Cl2	97.55(5)
Cl1−Fe1−N1	100.5(1)	Cl4−Fe2−N8	106.7(1)	Cl1−Fe−N1	91.01(11)
Cl1−Fe1−N2	168.1(1)	Cl4−Fe2−N6	172.4(1)	Cl1−Fe−N2	166.51(10)
Cl1−Fe1−N3	108.3(1)	Cl4−Fe2−N7	102.8(1)	Cl1−Fe−N3	98.43(12)
Cl1−Fe1−N4	94.6(1)	Cl4−Fe2−N5	95.4(1)	Cl1−Fe−N4	88.77(10)
Cl2−Fe1−N1	91.6(1)	Cl3−Fe2−N8	88.6(1)	Cl2−Fe−N1	166.11(10)
Cl2−Fe1−N2	89.8(1))	Cl3−Fe2−N6	88.2(1)	Cl2−Fe−N2	95.68(10)
Cl2−Fe1−N3	88.0(1)	Cl3−Fe2−N7	92.3(1)	Cl2−Fe−N3	93.60(12)
Cl2−Fe1−N4	162.2(1)	Cl3−Fe2−N5	164.5(1)	Cl2−Fe−N4	119.13(10)
N1−Fe1−N2	74.0(1)	N6−Fe2−N8	75.6(1)	N1−Fe−N2	76.52(14))
N1−Fe1−N3	150.7(2)	N7−Fe2−N8	150.0(1)	N1−Fe−N3	74.26(15)
N1−Fe1−N4	94.0(1)	N5−Fe2−N8	81.9(1)	N1−Fe−N4	71.77(13)
N2−Fe1−N3	76.7(1)	N6−Fe2−N7	74.5(1)	N2−Fe−N3	83.31(16))
N2−Fe1−N4	75.6(1)	N5−Fe2−N6	77.6(1)	N2−Fe−N4	82.49(14)
N3−Fe1−N4	78.9(1)	N5−Fe2−N7	89.9(1)	N3−Fe−N4	145.36(15)

X-ray Crystal Structure Analysis. $L_1Fe^{II}Cl_2$ and $L_2Fe^{II}Cl_2$. $L_1Fe^{II}Cl_2$ crystallizes with two molecules in the asymmetric unit. These two molecules, *a* and *b*, do not significantly differ, and selected bond lengths and angles for $L_1Fe^{II}Cl_2$ (*a* and *b*) and $L_2Fe^{II}Cl_2$ are given in Table 1. As shown in Figure 2, for both compounds the tripodal ligand coordinates in the standard tetradentate fashion. The two chloride atoms are bound to the metal, which lies in a distorted octahedral environment. The trans ligand angles display values below 180° with, for $L_1Fe^{II}Cl_2$ (*a*), values of 168.1(1)° for ∠Cl1−Fe1−N2, 162.2(1)° for ∠Cl2−Fe1−N4, and 150.7(2)° for ∠N1−Fe1−N3. The angles between Cl1 and its neighbors are significantly larger than 90° with ∠Cl1−Fe1−N1 = 100.5(1)°, ∠Cl1−Fe1−N3 = 108.3(1)°, and ∠Cl1−Fe1−N4 = 94.6(1)°. The value for ∠Cl1−Fe−Cl2 is 100.99(6)°. The flexibility of the ligand is expressed

(22) Cromer, D. T.; Waber, J. T. *International Tables for X-ray Crystallography*; The Kynoch Press: Birmingham, 1974; Vol. IV; (a) Table 2.2b; (b) Table 2.3.1.

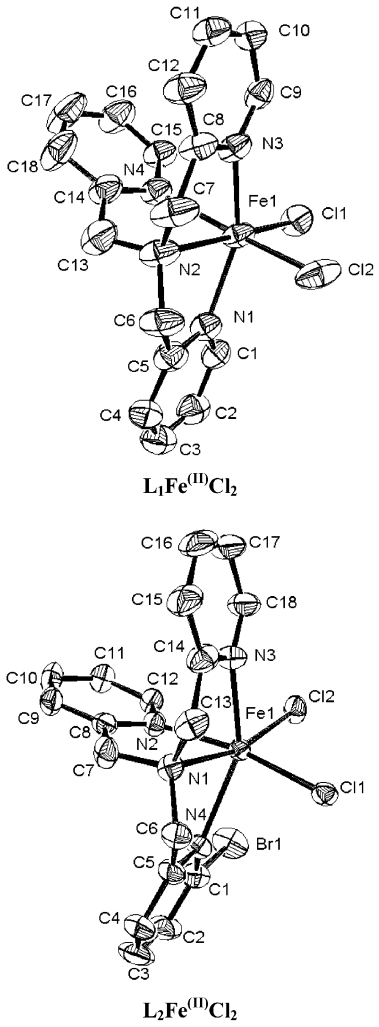

Figure 2. ORTEP diagrams of the six-coordinate $L_nFe^{II}Cl_2$ complexes.

by the small angles between the nitrogen atoms, with 74.0(1)° for ∠N1−Fe1−N2, 76.7(1)° for ∠N2−Fe1−N3, and 75.6(1)° for ∠N2−Fe1−N4. In general, in already reported structures of iron complexes of TPAs, the Fe−N(pyridine) bonds are shorter than the Fe−N(amine) one.[16,13,18] Indeed, the values of 2.183(4) and 2.180(4) Å found for *d*(Fe1−N3) and *d*(Fe1−N1), respectively, are shorter than the distance *d*(Fe1−N2) = 2.274(4) Å. But surprisingly, *d*(Fe1−N4) = 2.283(4) Å, which is high, presumably because of a trans effect with the chloride Cl2.

For L_1FeCl_2, the two trans pyridines are tightly bound to the metal. As a consequence and because of the steric hindrance provided by the chlorides, the N4−Fe distance is elongated, and the axial pyridyl ring is tilted with respect to the normal to the N1−N2−N3 plane. This additional distortion to the octahedral geometry is reflected by the values of the angles ∠N3−Fe−N4 and ∠N1−Fe−N4, which are respectively 78.9° and 93.9°, i.e., significantly different one from the other.

In $L_2Fe^{II}Cl_2$, similar general patterns are observed, the geometry being here again distorted from ideal octahedral, with trans ligand angles of 166.51(10)° for ∠Cl1−Fe−N2, 166.11(10)° for ∠Cl2−Fe−N1, and 145.36(15)° for N3−Fe−N4. The distortion is expressed by chloride-to-nitrogen angles larger than 90° with, for instance, ∠Cl2−Fe−N4 = 119.13(10)°, and by small nitrogen-to-nitrogen angles, with, for example, ∠N1−Fe−N4 = 71.77(13)°. The distance *d*(Fe−N1) = 2.302(4) Å is larger than the values of 2.248(4) and 2.169(4) Å observed for *d*(Fe−N3) and *d*(Fe−N2), respectively. The long distance of 2.354(4) Å for *d*(Fe−N4) may, in that case, be due to the steric repulsion between the α-brominated pyridine and the chloride ligands (vide infra). In L_2FeCl_2, the Fe−N4 distance is elongated because of steric repulsions between the bromine atom and the chloride ligands. Indeed, a distance of 3.679 Å between Br1 and Cl2 indicates that these two atoms are in van der Waals contact. As a consequence, the axial pyridine lies more symmetrical than in L_1FeCl_2, with ∠N3−Fe−N2 and ∠N4−Fe−N2 angles respectively of 83.3° and 82.5°. The shortest iron-to-nitrogen distance becomes *d*(Fe−N2), i.e., the one between the metal and the pyridine trans to the chloride. Finally, in this structure, the bromo-substituted pyridine is located laterally with respect to the Fe−Cl1−Cl2 plane. Van der Waals contacts are found between the bromine atom and the neighboring pyridine with the distances *d*(C12−Br1) = 3.919 Å and *d*(N2−Br1) = 3.536 Å. This unsymmetrical geometry certainly reflects a gain in stability.

Table 2. Selected Bond Lengths (Å) and Angles (deg) for the Five-Coordinate $L_nFe^{II}Cl_2$ Complexes

$L_3Fe^{II}Cl_2$		$L_4Fe^{II}Cl_2$	
Fe−Cl1	2.298(2)	Fe−Cl1	2.290(1)
Fe−Cl2	2.303(2)	Fe−Cl2	2.333(1)
Fe−N1	2.246(7)	Fe−N1	2.258(3)
Fe−N2	2.229(8)	Fe−N2	2.186(4)
Fe−N4	2.188(6)	Fe−N4	2.213(3)
Cl1−Fe−Cl2	130.8(1)	Cl1−Fe−Cl2	134.74(5)
Cl1−Fe−N1	95.2(2)	Cl1−Fe−N1	95.9(1)
Cl1−Fe−N2	114.4(2)	Cl1−Fe−N2	116.0(1)
Cl1−Fe−N4	94.8(2)	Cl1−Fe−N4	93.8(1)
Cl2−Fe−N1	98.7(2)	Cl2−Fe−N1	96.6(1)
Cl2−Fe−N2	114.7(2)	Cl2−Fe−N2	109.2(1)
Cl2−Fe−N4	93.8 (2)	Cl2−Fe−N4	93.2(1)
N1−Fe−N2	76.8(3)	N1−Fe−N2	78.0(1)
N1−Fe−N4	152.7(3)	N1−Fe−N4	154.6(1)
N2−Fe−N4	76.0(3)	N2−Fe−N4	76.6(1)

$L_3Fe^{II}Cl_2$ and $L_4Fe^{II}Cl_2$. The striking features in the structures of both compounds are (i) the tridentate coordination mode of the ligand, one substituted pyridine remaining out of the coordination sphere; and (ii) the pentacoordination of the metal which lies in a distorted trigonal bipyramidal geometry. Selected bond lengths and angles for $L_3Fe^{II}Cl_2$ and $L_4Fe^{II}Cl_2$ are given in Table 2, and ORTEP diagrams in Figure 3.

For $L_3Fe^{II}Cl_2$, the in-plane angles are ∠N2−Fe−Cl2 = 114.7(2)°, ∠N2−Fe−Cl1 = 114.4(2)°, and Cl1−Fe−Cl2 = 130.8(1)°. The ∠N1−Fe−N4 angle has a small value of 152.7(3)°. The distortion with respect to ideal trigonal bipyramidal geometry is also expressed by small ∠N2−Fe−N4 and ∠N2−Fe−N1 angles of 76.0(3)° and 76.8(3)°, respectively. The metal-to-chloride distances are *d*(Fe−Cl1) = 2.298(2) Å and *d*(FeCl2) = 2.303(2) Å. Other distances are *d*(Fe−N2) = 2.229(8) Å and *d*(Fe−N4) = 2.188(6) Å.

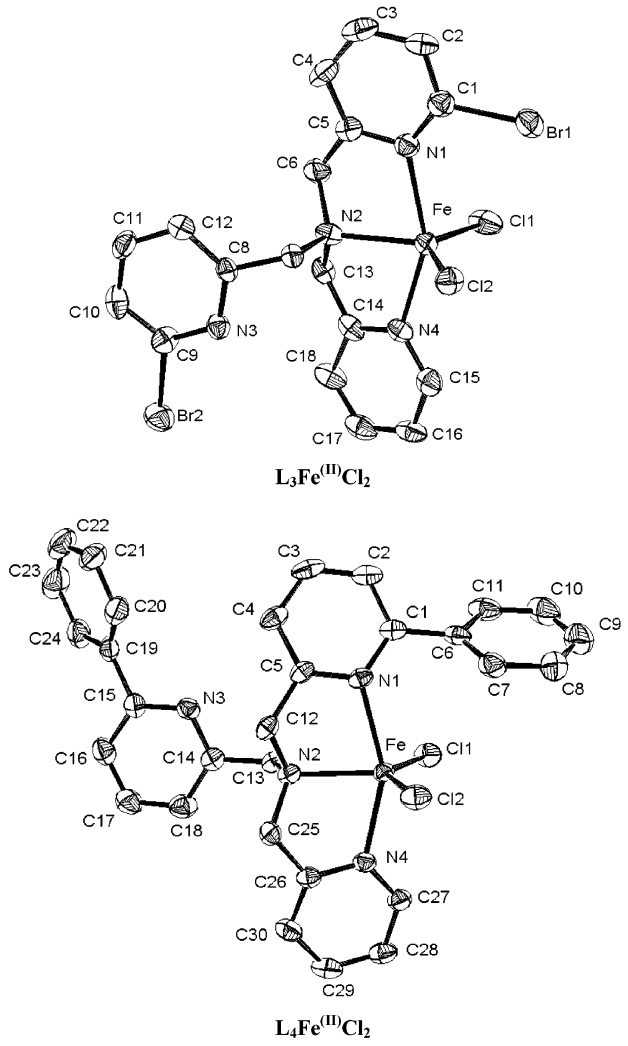

Figure 3. ORTEP diagrams of the five-coordinate $L_nFe^{II}Cl_2$ complexes.

The value d(Fe−N1) = 2.246(7) Å is high because of steric repulsions between the bromine atom of the substituted pyridine and the chloride ligands: indeed, the distances d(Br1−Cl1) and d(Br1−Cl2) are very short, with values of respectively 3.880 and 3.815 Å, indicating that these halogen atoms are in van der Waals contact. Under these conditions, hexacoordination by another bromopyridyl arm is impossible.

In $L_4Fe^{II}Cl_2$, the in-plane angles are ∠N2−Fe−Cl2 = 109.2(1)°, ∠N2−Fe−Cl1 = 116.0(1)°, and Cl1−Fe−Cl2 = 134.74(5)°. The ∠N1−Fe−N4 angle has a small value of 154.6(1)°. Small angles ∠N2−Fe−N4 = 76.6(1)° and ∠N2−Fe−N1 angles of 78.0(1)° reflect the distortion of the ligand. The metal-to-chloride distances are d(Fe−Cl1) = 2.290(1) Å and d(FeCl2) = 2.333(1) Å. The shortest Fe−N distance in this compound is d(Fe−N2) = 2.186(4) Å. The metal-to-pyridine bonds are longer, with values of d(Fe−N4) = 2.213(3) Å and d(Fe−N1) = 2.258(3) Å. Again in this structure, the phenyl substituent lies very close to the chloride ligands with the contacts d(C11−Cl1) = 3.836 Å, d(C7−Cl1) = 3.891 Å, and d(C7−Cl2) = 3.595 Å.

It is noteworthy that both compounds have been recrystallized in a mixture of diethyl ether and acetonitrile. Indeed, for $L_4Fe^{II}Cl_2$, both solvents are present in the unit cell, but despite their small sizes, they do not bind to the metal.

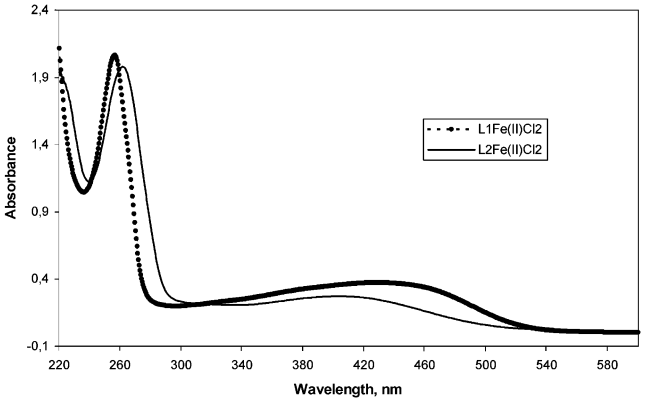

Figure 4. UV−visible spectra of $L_1Fe^{II}Cl_2$ and $L_2Fe^{II}Cl_2$ in CH_3CN.

Table 3. UV−Visible Absorption Maxima for the $L_nFe^{II}Cl_2$ Complexes

complex	wavelength, λ_{max}, nm (ϵ, 10^{-3} $mmol^{-1}\cdot cm^2$), CH_3CN, rt	
$L_1Fe^{II}Cl_2$	256.0 (8.35)	427.0 (1.44)
$L_2Fe^{II}Cl_2$	261.0 (7.52)	403.5 (1.03)
$L_3Fe^{II}Cl_2$	262.5 (sh), 269.0 (10.43), 276.0 (sh)	373.0 (0.62)
$L_4Fe^{II}Cl_2$	246.0 (17.90), 283.5 (17.03)	387.0 (0.65)

UV−Visible Spectroscopy. The absorption maxima for all complexes are listed in Table 3.

$L_1Fe^{II}Cl_2$ and $L_2Fe^{II}Cl_2$. The spectra of the six-coordinate compounds are displayed in Figure 4. They are dominated by a ligand-centered $\pi-\pi^*$ transition in the UV region, and by a broad and prominent transition in the near visible. For instance, for $L_1Fe^{II}Cl_2$, values of λ = 256.0 and 427.0 nm are found. We first thought that the broad absorption in the visible might be assigned as a charge-transfer transition from the coordinated chloride to the metal. But our data should be compared to those reported with some ferrous complexes with *N*,*N*,*N*′-tris(2-pyridylmethyl)ethane-1,2-diamine type ligands.[23] In such complexes, a similar broad band at 400 nm is assigned to a MLCT between the Fe(II) "$t2_g$" orbitals and the π^* pyridine orbitals, this assignment being based on overlap considerations. The origin of the absorptions in our series of compounds might be the same. The spectrum of $L_2Fe^{II}Cl_2$ looks very similar, with however a small weakening and shift of the broad band from λ = 427 nm in $L_1Fe^{II}Cl_2$ to λ = 403 nm in $L_2Fe^{II}Cl_2$.

$L_3Fe^{II}Cl_2$ and $L_4Fe^{II}Cl_2$. In the five-coordinate complexes, ligand-centered $\pi-\pi^*$ transitions are also observed in the UV region. In $L_4Fe^{II}Cl_2$, absorptions appear at λ = 246.0 and 283.5 nm and are split as a result of phenyl conjugation in the ligand. But the striking feature in both complexes, the spectra of which are similar in the visible range, is the significant weakening of the broad absorptions. Also, these weak signals are blue shifted with respect to those in the six-coordinate complexes, with, for example, in $L_4Fe^{II}Cl_2$, a maximum at λ = 387.0 nm. The spectra are shown in Figure 5. Obviously, the noticeable difference between $L_1Fe^{II}Cl_2$

(23) Mialane, P.; Nivorojkine, A.; Pratviel, G.; Azema, L.; Slany, M.; Godde, F.; Simaan, A.; Banse, F.; Kargar-Grisel, T.; Bouchoux, G.; Sainton, J.; Horner, O.; Guilhem, J.; Tchertanova, L.; Meunier, B.; Girerd, J.-J. *Inorg. Chem.* **1999**, *38*, 1085−1092.

Table 4. ^{1}H NMR Chemical Shifts and T_1 Relaxation Times for the Six-Coordinate $L_nFe^{II}Cl_2$ Complexes

	chemical shift, δ, ppm, CD_3CN, rt (T_1, ms)						
complex	α	$\beta_1-\beta_3,\beta_2$	$\beta'_1-\beta'_3,\beta'_2$	$\gamma_1-\gamma_3,\gamma_2$	CH_2	CH_2	CH_2
$L_1Fe^{II}Cl_2$	130 (0.20)	51.3, 50.5 (6.95, 4.18)	46.4, 45.8 (4.63, 3.79)	25.2, 24.8 (11.83, 6.40)	42 (very broad)		0.5 (2H) (0.78)
	α	β_{2-3},β'_{2-3}	β_1,β'_1	γ_{2-3},γ_1	CH_2	CH_2	CH_2
$L_2Fe^{II}Cl_2$	119 (0.46)	51.1, 44.4 (6.52, 4.01)	35.6, 23.3 (6.52, 2.40)	13.1, 11.0 (9.76, 14.2)	62 (0.42)	55 (0.88)	31 (0.49)

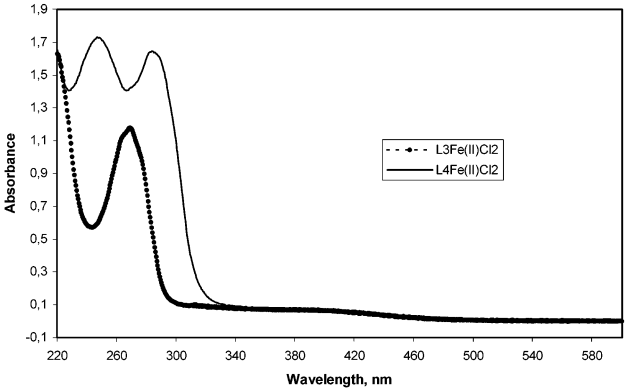

Figure 5. UV−visible spectra of $L_3Fe^{II}Cl_2$ and $L_4Fe^{II}Cl_2$ in CH_3CN.

and $L_2Fe^{II}Cl_2$ on one hand and $L_3Fe^{II}Cl_2$ and $L_4Fe^{II}Cl_2$ on the other hand reflects a difference in the ligand field around the metal and by consequence a difference in the coordination sphere. Considering the origin of the broad band as an MLCT between the Fe(II) "$t2_g$" orbitals and the π^* pyridine orbitals, its weakening in $L_3Fe^{II}Cl_2$ and $L_4Fe^{II}Cl_2$ complexes suggests that the tridentate mode of the ligand, with only two bound pyridines, is retained in solution.

^{1}H NMR. $L_1Fe^{II}Cl_2$ and $L_2Fe^{II}Cl_2$. The spectra are typical for high-spin ferrous complexes, and all resonances are listed in Table 4. All the signals have been assigned on the basis of the integrals and T_1 relaxation times, and the traces are shown in Figure 6. In $L_1Fe^{II}Cl_2$ the α protons of the coordinated arms are found at $\delta = 130$ ppm with a low value of $T_1 = 0.20$ ms. The β protons of the coordinated arms appear as sharp signals at $\delta = 51.3$, 50.5, 46.4, and 45.8 ppm ($T_1 = 6.95$, 4.18, 4.63, and 3.79 ms), and the γ protons at $\delta = 25.2$ and 24.8 ppm ($T_1 = 11.83$ and 6.40 ms). In trichloroferric complexes, the methylene protons are not visible on the spectra.[18] In the present case, we observe a broad signal integrating for two protons at 0.5 ppm and assign it to two of the six methylene protons, with a T_1 value of 0.78 ms. The presence of an extremely broad and weak band lying between 60 and 20 ppm on the spectrum may account for the remaining four methylene protons. In $L_2Fe^{II}Cl_2$ the two α protons of the coordinated pyridines appear at $\delta = 119$ ppm with $T_1 = 0.46$ ms. The β and β' protons of the unsubstituted pyridines are found at $\delta = 51.1$ and 44.4 ppm ($T_1 = 6.52$ and 4.01 ms) and are downfield shifted with respect to the β and β' protons of the bromo-substituted arm, which resonate at $\delta = 36.5$ and 23.3 ppm ($T_1 = 6.52$ and 2.40 ms). Three broad bands with short T_1 values are found at $\delta = 62$ (0.42 ms), 55 (0.88 ms), and 31 (0.49 ms) ppm and are assigned to the three methylene protons. Finally, the spectrum is very well resolved, and the fact that the

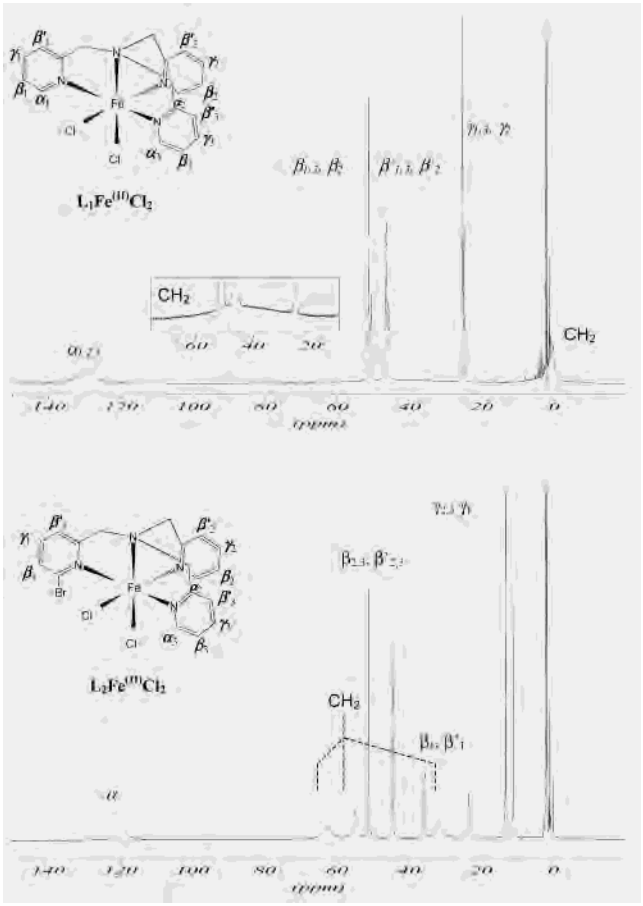

Figure 6. ^{1}H NMR spectra of $L_1Fe^{II}Cl_2$ and $L_2Fe^{II}Cl_2$ in CD_3CN.

methylene protons appear as three distinct signals strongly supports that the geometry around the metal found in the solid state is also retained in solution.

$L_3Fe^{II}Cl_2$ and $L_4Fe^{II}Cl_2$. The spectra of the complexes also reflect a high-spin state for the metal, with broader signals than those observed in the above-described compounds (Figure 7, Table 5). In $L_3Fe^{II}Cl_2$, four signals display very short relaxation times. The unique α proton of the coordinated pyridine appears at $\delta = 123$ ppm with $T_1 = 0.12$ ms. Then, three signals corresponding to two protons each are found at $\delta = 72$ ($T_1 = 0.42$ ms), 34 ($T_1 = 0.74$ ms), and 20 ppm ($T_1 = 0.76$ ms) and are assigned to the methylene protons. Two other signals with relaxation times close to each other are found at $\delta_a = 55.5$ ppm ($T_{1a} = 1.15$ ms) and $\delta_b = 0.7$ ppm ($T_{1b} = 0.95$ ms). They certainly correspond to the β, β', and γ protons of the coordinated pyridines. Considering the relaxation times only, δ_b would fit to the β and β' and δ_a to the γ protons. However, the difference in these values might be not significant with

Table 5. ^{1}H NMR Chemical Shifts and T_1 Relaxation Times for the Five-Coordinate $L_nFe^{II}Cl_2$ Complexes

	chemical shift, δ, ppm, CD_3CN, rt (T_1, ms)				
complex	α	CH_2	phenyl subst (L_4)[a]	uncoord Py	β, β', and γ
$L_3Fe^{II}Cl_2$	123	72, 34, 20		6.3, 4.0	55.5, 0.7
	(0.12)	(0.42, 0.74, 0.76)		(1.98, 2.08)	(1.15, 0.95)
$L_4Fe^{II}Cl_2$	120	88, 31, 21	10.8, 7.0, 4.8	2.1, 1.8	54.1, 52.9, 7.5, 4.5
	(0.13)	(0.17, 0.31, 0.34)	(0.98, 5.79, 2.17)	(6.0, shoulder)	(2.08, 1.37, 1.0, 1.1)

[a] δ values from ^{2}H NMR on $[Ph_2d^{10}]L_4Fe^{II}Cl_2$

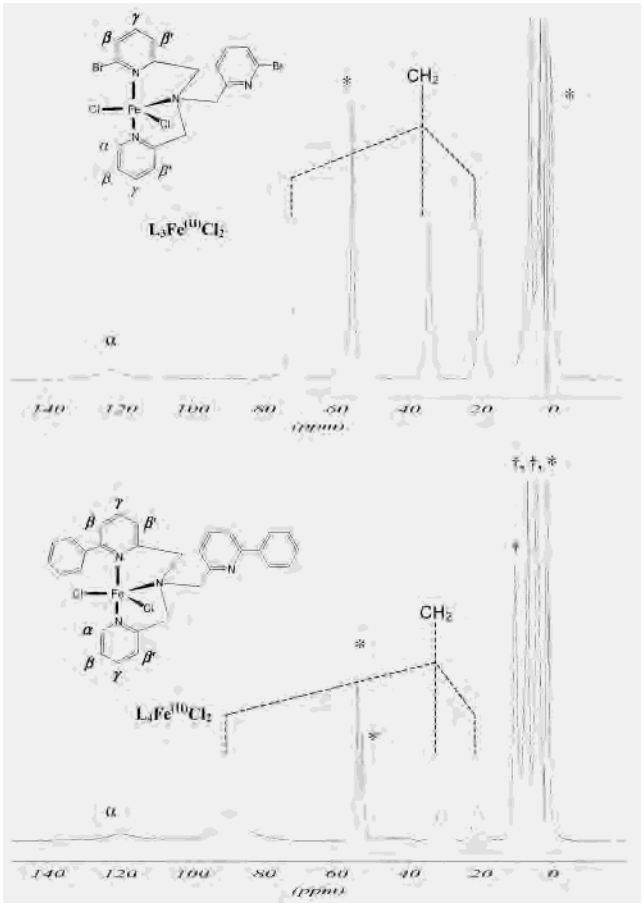

Figure 7. ^{1}H NMR spectra of $L_3Fe^{II}Cl_2$ and $L_4Fe^{II}Cl_2$ in CD_3CN: (*) β, β', and γ protons; (†) phenyl substituent of the pyridine (L_4).

respect to the experimental errors. Finally, the only remaining signals on the spectrum are found in the diamagnetic region, at $\delta = 6.3$ ($T_1 = 1.98$ ms) and 4.0 ppm ($T_1 = 2.08$ ms), and are attributed to the protons of the uncoordinated pyridine. The spectrum of $L_4Fe^{II}Cl_2$ also displays four signals with short T_1 values. The broad resonance at $\delta = 120$ ppm, $T_1 = 0.13$ ms is assigned to the α proton of the coordinated pyridine. The methylene signals are found at $\delta = 88$, 31, and 21 ppm and with $T_1 = 0.17$, 0.31, and 0.34 ms. The diamagnetic region should contain the signals from the uncoordinated pyridine, together with those of the phenyl substituents. The resonance of these phenyl protons has been unequivocally assigned using ^{2}H NMR on the selectively deuterated $[Ph_2d^{10}]TPAFe^{II}Cl_2$ complex. The spectrum, available as Supporting Information, shows that, for this complex, these protons give rise to three signals at $\delta = 10.8$ (0.98 ms), 7.0 (5.79 ms), and 4.8 ppm (2.17 ms).[27] Other signals in the diamagnetic region with $\delta = 2.1$ (6.00 ms) and 1.8 ppm (shoulder in CD_3CN) are assigned to the protons of the uncoordinated pyridine. Finally, the remaining resonances display short to moderate T_1 and appear at $\delta = 54.1$ ppm (2.08 ms), 52.9 ppm (1.37 ms), 7.5 (1.01 ms), and 4.5 (1.09 ms). They might account for the β, β', and γ protons of the coordinated pyridine, with a noticeable difference in chemical shifts and relaxation times due in part to the presence of one phenyl ring on the coordinated pyridine.

Furthermore, the coordination of acetonitrile to the metal has been considered in $L_3Fe^{II}Cl_2$ and $L_4Fe^{II}Cl_2$. Thus, aliquots of CH_3CN in solution in the deuterated solvent have been added to NMR solutions of the complexes. However, no modification of the spectra could be observed.

Conductivity Measurements. Whereas tetradentate coordination mode of the ligand in solutions of $L_1Fe^{II}Cl_2$ and $L_2Fe^{II}Cl_2$ may be deduced from ^{1}H NMR data, the question arises for $L_3Fe^{II}Cl_2$ and $L_4Fe^{II}Cl_2$. We have measured the molecular electric conductivities of all complexes in acetonitrile, at concentrations close to that used for NMR experiments. We found for each of them very similar values, close to 30×10^6 $\mu S \cdot cm^2 \cdot mol^{-1}$, as shown in Table 6. Our data may be compared to those reported with some dichloro iron and manganese complexes with tetraazamacrocycles which have been shown to remain neutral in solution.[24] For these macrocyclic iron complexes, the values lie between 47 and 62×10^6 $\mu S \cdot cm^2 \cdot mol^{-1}$. We thus have evidence that our compounds remain neutral in solution. But additional support maybe obtained by comparison of our data with those obtained from charged species. Two easy ways lead to the formation of cationic complexes: following already known procedures, mixing a 1:1 equivalent of ligand and metal dichloride in the presence of weakly coordinating anions is expected to yield a dinuclear dicationic species.[15] But also possible is the formation of mononuclear dications by mixing a 2:1 mixture of ligand and chloride-free salt.[13] We thus generated cationic species by addition under inert atmosphere of a 2:1 equivalent of ligand to the $Fe^{II}(BF_4)_2$. Using this procedure, species are obtained the molecular conductivities of which lie all together in the same range. However, the

(24) Hubin, T. J.; McCormick, J. M.; Collinson, S. R.; Buchalova, M.; Perkins, C. M.; Alcock, N. W.; Kahol, P. K.; Raghunatan, A.; Busch, D. H. *J. Am. Chem. Soc.* **2000**, *122*, 2512−2522.

(25) Britovsek, G. J. P.; Gibson, V. C.; Kimberley, B. S.; Mastroianni, S.; Redshaw, C.; Solan, G. A.; White, A. J. P.; Williams, D. J. *J. Chem. Soc., Dalton Trans.* **2001**, 1639−1644.

(26) Britovsek, G. J. P.; Bruce, M.; Gibson, V. C.; Kimberley, B. S.; Maddox, P.; Mastroianni, S.; McTavish, S. J.; Redshaw, C.; Solan, G. A.; Strömberg, S.; White, A. J. P.; Williams, D. J. *J. Am. Chem. Soc.* **1999**, *121*, 8728−8740.

(27) All T_1 values of well-defined signals have been measured on the regular nondeuterated $L_4Fe^{II}Cl_2$ complex. The signals at $\delta = 7.5$ and 4.5 ppm appear as shoulders within the phenyl peaks; their T_1 values were obtained from measurements on the phenyl-deuterated complex for which they appear as single peaks.

Table 6. Molecular Conductivities Observed in Acetonitrile at 20 °C for All Complexes Described in This Study[a]

complex	concn, mmol·L^{-1}	blank cell conductivity, μS·cm^{-1}	sample conductivity, μS·cm^{-1}	sample − blank conductivity, μS·cm^{-1}	molar conductivity, 10^6 μS·cm^2·mol^{-1}
$L_1Fe^{II}Cl_2$	3.60	2.1	109.2	107	29.7
$L_2Fe^{II}Cl_2$	3.02	1.6	92.1	90	29.8
$L_3Fe^{II}Cl_2$	2.61	1.3	86.5	85	32.5
$L_4Fe^{II}Cl_2$	2.63	1.5	76.9	75	28.5
$Fe^{II}(BF_4)_2 + L_1$	3.80	1.7	582.0	580	152.6
$Fe^{II}(BF_4)_2 + L_2$	3.80	1.6	572.1	570	150.0
$Fe^{II}(BF_4)_2 + L_3$	3.80	1.3	551.3	550	144.7
$Fe^{II}(BF_4)_2 + L_4$	3.80	2.0	552.2	550	144.7

[a] Lines 5−8: Anaerobic solutions of $Fe^{II}(BF_4)_2$ under argon in which a 2-fold excess of ligand is added. Equilibration time of 5 min after appearance of the yellow color, then measurement.

values found for these compounds are close to 150×10^6 μS·cm^2·mol^{-1}, i.e., much higher than those measured on the complexes, and strongly support in that specific case the presence of charged species in solution.

In consequence, we believe that all complexes $L_{1-4}Fe^{II}Cl_2$ described in this study remain neutral molecules in acetonitrile solution.

Discussion

In general, coordination of exogenous ligands to ferrous TPA derivatives is limited to either biomimetic anions (acetates, thiolates, or catechols, for example) or weakly coordinating anions.[13−17] In this study, the choice of chloride ions, which in organic solvents are strongly coordinating, was dictated by the need to obtain complexes displaying excellent criteria of stability in various media. The preparation is very simple, and by contrast to other methods involving mixtures of chloride, perchlorate, and boron-substituted counterions from which bis(μ-halo) diiron(II) complexes can be prepared, we obtained mononuclear complexes.[15] With the parent TPA ligand L_1 and the monobrominated (BrTPA)L_2, low or limited steric constraints allow tetradentate coordination of the tripod ligand to $Fe^{II}Cl_2$. By contrast, with the di-α substituted tripods L_3 and L_4, decoordination of one substituted pyridyl arm occurs, leaving the metal in a five-coordinate geometry, even in the presence of a potentially coordinating solvent such as acetonitrile. In chemistry of iron complexes, precedents of tridentate coordination of TPA derivatives are known in both ferric and ferrous states.[13,16,18] Decoordination of a pyridyl arm generally occurs because of steric repulsions around the metal. This is the case with ligands substituted in the α position of the pyridyl arm(s), or in complexes in which two tripods coordinate to a single metal atom. The geometry around the metal in complexes $L_3Fe^{II}Cl_2$ and $L_4Fe^{II}Cl_2$ is more unusual. Trigonal bipyramidal geometry has been reported in ferrous derivatives with thiophenolato ligands, but in these cases the tripod acts as a tetradentate ligand.[14] To our knowledge, the only precedent for a trigonal bipyramidal environment in which a TPA ligand coordinates the iron in a tridentate way has been described in the ferric derivative $[(6\text{-}Me_3TPA)Fe(NO)_2](ClO_4)_2$.[16] Small nitrosyl ligands bind to the metal, but substitution at the *three* pyridyl arms prevents complete folding of the tripod. From a more general point of view, a few examples of dichloro iron complexes with trigonal bipyramidal geometries can be found with imido type ligands and are generally studied in the field of polymerization catalysis.[25,26]

Simple ferrous complexes of TPA or its 6-methyl derivative have already been fully characterized, and the relationship between structure and spin state has been examined in detail.[3,13] Spin state is closely related to metal-to-ligand distances, and substitution at the α position by a methyl group has been shown to induce elongation of the metal-to-ligand bonds. In the present case all factors combine to give high-spin complexes: chloride ions are low-field ligands, and their size exerts enough steric constraint to push away the ligand from the metal, with no metal-to-ligand distances lower than 2.0 Å. ^{1}H NMR data on ferrous mono- or dinuclear complexes has already been reported.[3,6,7,13,14] Our ^{1}H NMR data also supports a high-spin state for the metal in all complexes with relaxation times lying between 0.1 and 7 ms for the paramagnetically shifted protons, i.e., which are in the lower limit of the range expected for Fe^{II} $S = 2$ systems.[3,13] Interestingly, the relaxation times are shorter in $L_3Fe^{II}Cl_2$ and $L_4Fe^{II}Cl_2$ than in the other complexes, which might reflect a different magnetic distribution around the coordination sphere. In early NMR studies of metal−pyridine complexes, pyridine protons were found to experience downfield shifts which attenuate in the order α-H > β-H > γ-H.[14] This has been interpretated as the result of a σ mechanism for delocalizing unpaired spin density. In this study, all α protons appear at low field with short relaxation times, in line with previously reported data on high-spin ferrous monomers for which in general the signals lie between 70 and 140 ppm. The assignment of the β and γ protons in the $L_1Fe^{II}Cl_2$ and $L_2Fe^{II}Cl_2$ complexes is straightforward and follows the general pattern.[3,6,7,13,14] But the question remains open in the five-coordinate complexes, where slightly shorter relaxation times (at least in the same order of magnitude) are found for the upfield signal.

The qualitative difference in the spectra of the six- and five-coordinate complexes should be considered in light of previously reported studies.[14] It has been shown that a σ delocalization is the only possibility left for the magnetic exchange between the metal orbitals and the pyridine ligands in the six-coordinate TPA complexes. But the question of π delocalization might arise in the case of the five-coordinate compounds with a trigonal bipyramidal geometry. Although $L_3Fe^{II}Cl_2$ and $L_4Fe^{II}Cl_2$ deviate from the ideal trigonal

bipyramidal geometry, some π delocalization might account for the shorter relaxation times in these complexes.[14]

Finally, the question of the conservation of the structure in solution may be important in view of further use of the complexes. We believe that tetradentate coordination is retained in solution for $L_1Fe^{II}Cl_2$ and $L_2Fe^{II}Cl_2$ complexes. With $L_3Fe^{II}Cl_2$ and $L_4Fe^{II}Cl_2$, both UV−visible spectroscopy and ^{1}H NMR support the retention of the structure in solution. Tetradentate coordination of the tripods L_3 and L_4 to undissociated $Fe^{II}Cl_2$ also seems to be extremely unlikely from crystallographic studies. However, it is not possible to rule out that, upon removal of at least one chloride atom from the metal, tetradentate refolding of the ligand might be possible, followed—or not—by coordination of an acetonitrile molecule. This would definitely afford charged species $[(L_nFe^{II}Cl)(CH_3CN)_x]^+$. Our electric conductivity measurements invalidate this hypothesis. We show that all complexes, upon solubilization in acetonitrile, display very low conductivities in a narrow range similar to those found in other neutral complexes;[24] furthermore, comparison with data obtained from related ionic complexes at similar concentrations strongly support that $L_{1-4}Fe^{II}Cl_2$ remain neutral in solution. Thus, tridentate coordination of the tripod in solutions of $L_3Fe^{II}Cl_2$ and $L_4Fe^{II}Cl_2$ is the only possibility left. Finally, the fact that the NMR spectra of $L_3Fe^{II}Cl_2$ and $L_4Fe^{II}Cl_2$ are not affected by the addition of aliquots of nondeuterated CH_3CN suggests that acetonitrile does not bind to the metal in solution, and that conservation of the structure of the solid state in solution is the most likely possibility.

In summary, we report in this article the preparation of a series of four dichloroferrous complexes with tripodal ligands, TPA or derivatives in which the α position of one or two pyridyl arms is substituted by a bromine or phenyl group. In addition to full characterization by X-ray crystallography and ^{1}H NMR and UV−visible spectroscopies, the most salient point of this study is to demonstrate that pentacoordination at the metal site occurs in dichloroferrous complexes with a modified TPA ligand in which two pyridyl arms are substituted in the α position, and that tridentate coordination of the tripod is very likely retained in solution. This property may be extremely useful when vacant coordination sites are needed at the vicinity of a reactive metal center. Extensive work in this direction is currently under investigation in our group.

Acknowledgment. The authors are indebted to Prof. J. Fischer, Dr. A. De Cian, and Mrs. N. Gruber from the Service Commun de Rayons X, Faculté de Chimie, Université louis Pasteur for the X-ray structural determinations. We thank also Prof. R. Louis for useful discussions about the conductivity experiments. Financial support by the CNRS and the ULP is gratefully acknowledged.

Supporting Information Available: Side view of the ORTEP diagrams for all complexes with selected angles and contacts. ^{1}H NMR spectrum of $L_4Fe^{II}Cl_2$ in the diamagnetic region. ^{2}H NMR spectrum of $[Ph_2d^{10}](TPA)Fe^{II}Cl_2$, CH_3CN, 295 K. Tables of crystallographic data and crystallographic files in CIF format for the four reported structures. This material is available free of charge via the Internet at http://pubs.acs.org.

IC011104T